European Journal of Medicinal Chemistry 62 (2013) 416–424

Contents lists available at SciVerse ScienceDirect

European Journal of Medicinal Chemistry

journal homepage: http://www.elsevier.com/locate/ejmech

Original article

New annelated thieno[2,3-*e*][1,2,3]triazolo[1,5-*a*]pyrimidines, with potent anticancer activity, designed through VLAK protocol

Antonino Lauria*, Ilenia Abbate, Chiara Patella, Annamaria Martorana, Gaetano Dattolo, Anna Maria Almerico

Dipartimento di Scienze e Tecnologie Biologiche Chimiche e Farmaceutiche "STEBICEF", Sezione di Chimica Farmaceutica e Biologica, Università di Palermo, Via Archirafi 32, I-90123 Palermo, Italy

ARTICLE INFO

Article history:
Received 28 November 2012
Received in revised form
10 January 2013
Accepted 13 January 2013
Available online 23 January 2013

Keywords:
Annelated thienotriazolopyrimidines
Domino reactions
VLAK protocol
Developmental Therapeutics Program (DTP)
Anticancer agents

ABSTRACT

Drug design was performed through the Virtual Lock-and-Key (VLAK) protocol. This *in silico* approach allowed to select new annelated thienotriazolopyrimidine derivatives, potentially antitumor drugs. Starting from benzothieno[2,3-*e*][1,2,3]triazolo[1,5-*a*]pyrimidine and Pyrido[3′,2′:4,5]thieno[2,3-*e*][1,2,3]triazolo[1,5-*a*]pyrimidine core structures, new derivatives of these nuclei were designed and synthesized. Three of them were selected by the Development Therapeutical Program (DTP) of the National Cancer Institute (NCI) for the anticancer screening against a panel of 60 human tumor cell lines. The biological results showed that the new derivatives exhibited an excellent antiproliferative activity reaching sub-micromolar concentration. Moreover, to be evidenced their low toxicity and high potency.

1. Introduction

For many decades the molecular descriptors were used in the Quantitative Structure–Activity/Property Relationships (QSAR/QSPR) in various field of chemistry [1–3]. One of the limits in the application of QSAR/QSPR models is the necessity to use structures with a common core. Thus, if a diversity set database, with useful biological data, is available, it is not usually possible to employ these data in such an approach, although in the past some attempt, by using molecular descriptors and multivariate analysis, was performed [4].

A method to bypass this limit is to use the molecular descriptors, rather than in QSAR, in chemometric protocols like that recently proposed by us in Virtual Lock-and-Key (VLAK) approach [5]. This one was defined as the "*in silico* son" of the famous Lock-and-Key model of Fischer [6–8].

The VLAK protocol consists in the building of an *in silico* lock for a biological target, starting from its own ligands. In particular, the complex biological target-ligand is considered like a Lock-and-Key system.

The lock, to be released, requires a key with a shape that is able to fit all the lock pins, in the same way a biological target to work needs suitable interactions with a specific ligand in the complex formation.

In the VLAK protocol, these interactions are represented by the molecular descriptors, the equivalent of the pins in a Lock-and-Key system (Fig. 1).

Thus, a structure can be considered a potential ligand of a biological target, if its molecular descriptor values fit those of the biological target. The protocol can be applied in all the cases in which biological data are available (inhibition of a biological target, mechanism of action, etc).

Another feature of the VLAK protocol is the capability to identify the molecular descriptors values which are relevant when the enhancement of a biological activity is detected. This approach could help in the selection of convenient substituent in the lead optimization process.

In a previous work the molecular modeling allowed to improve the anticancer activity of indolo[3,2-*e*][1,2,3]triazolo[1,5-*a*]pyrimidine derivatives (Fig. 2), through the insertion of selected moieties in the core structure [9]. In fact, when the derivative **1a**, inactive as

Abbreviations: ACAM, AntiCancer Mechanism of Action database; CDI, 1,1′-Carbonyldiimidazole; DMAP, 4-DiMethylAminoPyridine; DMF, *N*,*N*-DiMethylFormamide; DTP, Developmental Therapeutical Program; EDCI, 1-Ethyl-3-[3-DiMethylAminoPropyl]Carbodiimide; MG_MID, Mean Graph MIDpoint; NCI, National Cancer Institute of Bethesda (MD, USA); QSAR/QSPR, Quantitative Structure/Activity/Property Relationships; VLAK, Virtual Lock And Key.

* Corresponding author. Tel.: +39 0916167210; fax: +39 0916230923.
E-mail addresses: antonino.lauria@unipa.it, antonino.lauria@gmail.com (A. Lauria).

0223-5234/$ – see front matter © 2013 Elsevier Masson SAS. All rights reserved.
http://dx.doi.org/10.1016/j.ejmech.2013.01.019

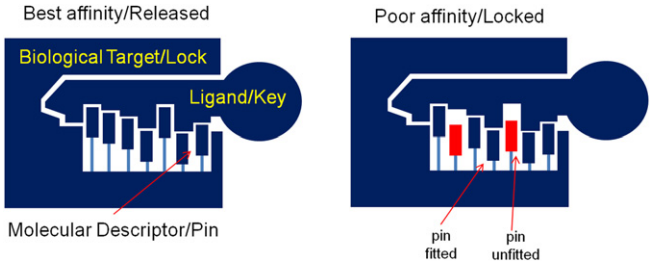

Fig. 1. Analogy Lock-and-Key and Biological Target-Ligand.

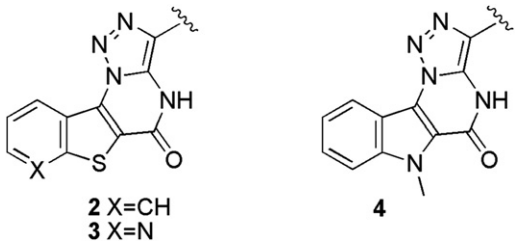

Fig. 3. Benzothieno[2,3-*e*][1,2,3]triazolo[1,5-*a*]pyrimidine **2**, Pyrido[3′,2′:4,5]thieno[2,3-*e*][1,2,3]triazolo[1,5-*a*]pyrimidine **3**, and indolo[2,3-*e*][1,2,3]triazolo[1,5-*a*]pyrimidine **4** core structures.

antitumor agent, was functionalized with side chains, selected on the basis of molecular modeling techniques, the anticancer activity has been increased (**1b**–**d**).

In this work, we propose the application of the VLAK protocol, at first to analyze the chemometric features, which are correlated with the increase of antitumor activity of the indolo[3,2-*e*][1,2,3]triazolo[1,5-*a*]pyrimidine derivatives **1**, and then to apply these findings in the lead optimization of new heterocyclic derivatives.

In previous works our experience in the synthesis of polyheterocyclic core structures led to the construction of various ring systems [10–17]. The most common synthetic approaches regarded the one step construction of new ring systems by starting from *ortho*-amino-cyano heterocycles and *N*-(BisMethylthio)Methylenamino Acids (BMMAs) [14], or from *ortho*-azido-carboxyethyl heterocycles and acetonitrile derivatives in domino 1,3-cycloaddition reactions [10–13], or by using the bis-cycloaddition of dipoles on annelated pyrazine derivatives [15–17].

2. Results and discussion

2.1. Chemometric protocol

In connection with our previous studies, devoted to the search of heterocyclic compounds with biological activities, and with the aim to exploit further the domino reaction involving derivatives *ortho*-azido-carboxyethyl heterocyclic systems and acetonitriles, we planned to synthesize the cores benzothieno[2,3-*e*][1,2,3]triazolo[1,5-*a*]pyrimidine **2** and pyrido[3′,2′:4,5]thieno[2,3-*e*][1,2,3]triazolo[1,5-*a*]pyrimidine **3** (Fig. 3).

They represent the thio and aza-thio isosteres of the core indolo[2,3-*e*][1,2,3]triazolo[1,5-*a*]pyrimidine **4**, previously synthesized by us [12]. The core structure of type **3** is known in literature [18], while the type **2** is a new ring system. The attention on the rings of type **2** and **3** was driven by the interest of studying new annelated triazolo[1,5-a]pyrimidines having a different ring fusion and consequently an aromatic feature different from the previously studied *nucleus* (Fig. 2).

The synthetic methodology involves a domino reaction between the ethyl 3-azido-benzo[*b*]thiophene-2-carboxylate (**5**) or the aza analog ethyl 3-azidothieno[2,3-*b*]pyridine-2-carboxylate (**6**) and acetonitriles **7** (Scheme 1).

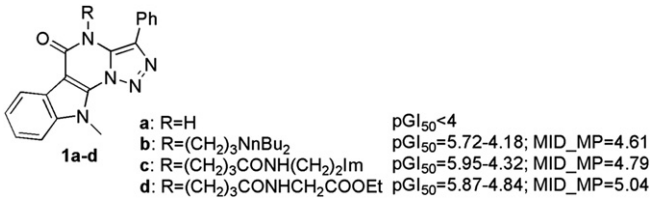

Fig. 2. Antiproliferative activity of indolo[3,2-*e*][1,2,3]triazolo[1,5-*a*]pyrimidine derivatives.

The first step involves 1,3-cycloaddition reactions in which the dipolar components are the 3-azido derivatives **5** and **6**, prepared from the corresponding amino derivatives **8** and **9**, respectively (Scheme 2).

The ethyl 3-aminobenzo[*b*]thiophene-2-carboxylate (**8**) is commercially available (CAS 34761-09-6), whereas the ethyl 3-aminothieno[2,3-*b*]pyridine-2-carboxylate (**9**) was obtained from 2-chloro-3-cyanopyridine and ethyl thioglycolate as described in literature [19].

They were diazotized with sodium nitrite followed by the addition of sodium azide in acetic acid or hydrochloric acid 6 N at −5 °C, according to the classical method used for the preparation of azides (Scheme 2).

The azides **5** and **6** were added at room temperature to the sodium salt of acetonitriles **7** in dry ethanol (Scheme 1).

A particular behavior was observed in the reaction of **6** with malononitrile (**7b**). Only in this case it was possible to isolate the intermediate 3-[triazol-1-yl] compound **10** (X = N, R = CN) with the amino group and carboxylate functions unreacted. The isolation of this intermediate allowed to confirm the mechanism of these reactions, already proposed by us [9–12]. The subsequent intramolecular cyclization originated the pyrimidine ring; this process is strictly influenced by the amount of the solvent used in the reaction. In fact, smaller volume of dry ethanol allowed to isolate the compound **10** (X = N, R = CN) in good yield.

The synthesized compounds **2** and **3** were submitted to DTP NCI protocol and tested against a panel of 60 human tumor cell lines.

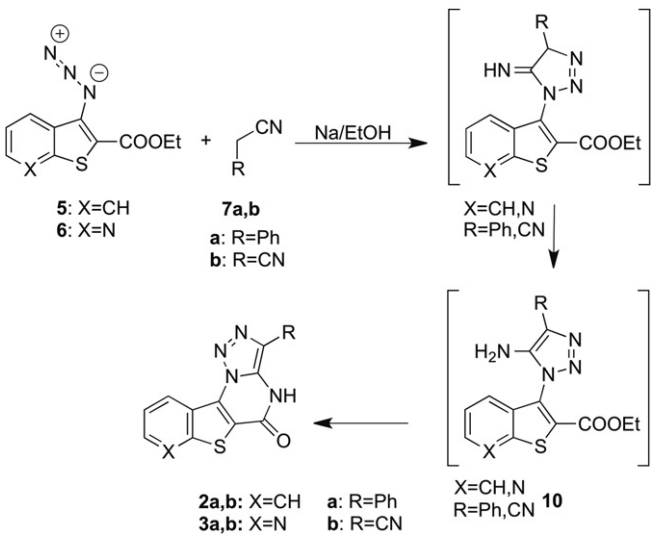

Scheme 1. Domino reaction leading to benzothieno[2,3-*e*][1,2,3]triazolo[1,5-*a*]pyrimidine **2** and Pyrido[3′,2′:4,5]thieno[2,3-*e*][1,2,3]triazolo[1,5-*a*]pyrimidine **3**.

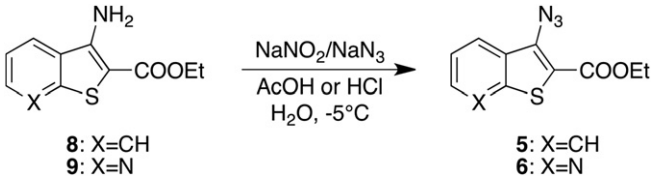

Scheme 2. Synthesis of ethyl 3-azido-benzo[*b*]thiophene-2-carboxylate (**5**) and ethyl 3-azidothieno[2,3-*b*]pyridine-2-carboxylate (**6**).

In the preliminary biological screenings, derivatives **2a**,**b** and **3a**,**b** showed poor antiproliferative activity, with a similar response in all panels (Table 1, Supplementary material).

These results are not surprising, since analogous behavior was already observed in the case of the indolo[3,2-*e*][1,2,3]triazolo[1,5-*a*]pyrimidine derivatives **1** [9].

With the aim to improve the biological activities of the new synthesized compounds, the VLAK protocol was applied to the annelated triazolo-pyrimidines **1** to verify which chemometric features contributed to antitumor activity increase (Fig. 2), and to take advantage of these findings in the lead optimization of **2** and **3**.

The first step of the VLAK protocol consists in the conversion of the biological target in a "lock model" in which the keys (the candidate ligands) could be "fitted" [5].

In this work we considered as biological targets the mechanism of action classes reported by the NCI in the AntiCancer Mechanism of Action (ACAM) database [20–22].

The ACAM database consists of 121 antitumor drugs classified according to their known mechanism of action (see Experimental section and Supplementary material).

Applying the VLAK protocol, each set of structures, related to a specific mechanism of action, is converted in a lock model.

The use of these models in the *in silico* screening of an external database could allow the identification of new structures, potentially correlated to a specific mechanism, that generates the lock model.

Recently we successfully applied this approach in the lead optimization of pyrrolo-pyrimidine derivatives as anticancer agents [23].

Thus, for each class of drugs (Alkylating Agents, Antimitotic Agents, Topoisomerase I Inhibitors, Topoisomerase II Inhibitors, RNA/DNA Antimetabolites, and DNA Antimetabolites), a "lock model" was built starting from known drugs (Experimental section).

The derivatives of type **1a**–**d** (Fig. 2) were submitted to "locks fitting" and the percentage of affinity (A%) for each derivative was calculated as reported in Experimental section (Table 2).

Table 1
Overview of cellular growth percentage average ($G\%_a$) of annelated benzothieno [2,3-*e*][1,2,3]triazolo[1,5-*a*]pyrimidine derivatives **2** and **3** against the nine DTP NCI sub-panels cancer cell lines.

PANEL	Derivative ([a]$G\%_a$)			
	2a	**2b**	**3a**	**3b**
Breast cancer	98.89	103.68	104.17	104.94
CNS cancer	110.45	101.13	103.98	104.07
Colon cancer	110.88	101.24	108.99	105.93
Leukemia	88.49	78.70	97.98	99.51
Melanoma	103.55	98.04	102.70	102.45
Non-small cell lung cancer	96.98	105.04	99.70	102.28
Ovarian cancer	97.38	103.11	102.12	106.50
Prostate cancer	96.49	99.82	105.18	104.38
Renal cancer	98.54	100.47	107.34	106.38

[a] cellular growth percentage average.

Table 2
VLAK results on indolo[3,2-*e*][1,2,3]triazolo[1,5-*a*]pyrimidines ([a]A%).

ID	[b]**MA**					
	A	**B**	**C**	**D**	**E**	**F**
1a	72	36	28	31	74	68
1b	30	95	43	95	48	29
1c	31	84	36	74	41	26
1d	33	94	46	94	50	32

[a] Percentage of affinity.
[b] **MA**, mechanism of action: **A**, Alkylating Agents; **B**, Antimitotic Agents; **C**, Topoisomerase I Inhibitors; **D**, Topoisomerase II Inhibitors; **E**, RNA/DNA Antimetabolites; **F**, DNA Antimetabolites.

The analysis of the VLAK results showed a predominant A% with the mechanism of action of classes **B** and **D**, respectively Antimitotic Agents and Topoisomerase II Inhibitors. The low A% values for the derivative **1a** (36 and 31) are on the line to the poor antiproliferative activity showed by the main core structure [9]. On the other hand, the **B** and **D** mechanisms reached the A% mean of 91 and 86, for derivatives **1b**–**d**. These high A% values underlines the deep influence of the side chains in the improvement of the biological activity.

On the basis of these remarks, an *in house* database was built considering the structures **2** and **3**, which were decorated by appropriate substituents in positions 4 (**A**–**L**) and 5 (**a**–**f**), (Fig. 4). The selection criteria of substituents were driven by different features: acidity, steric hindrance, and at least the guideline of the good biological results obtained for the indolo[3,2-*e*][1,2,3]triazolo [1,5-*a*]pyrimidine derivatives [9].

The *in house* database was submitted to VLAK protocol. In the Supplementary material the output results for all derivatives against the lock models representing each class of drugs (MAs) are reported. Table 3 reports the best ranked derivatives, expressed in percentage of affinity (A%), focusing on the mechanisms of action B and D, as suggested from the results obtained for the indolo[3,2-*e*] [1,2,3]triazolo[1,5-*a*]pyrimidines **1**.

Thus, the VLAK protocol led the selection of the derivatives **2aF**, **3aE**, **3aK** for the class B, and **3aF**, for the class D.

2.2. Chemistry

The synthesis of the compounds **2aF**, **3aE**, **3aK** and **3aF**, selected on the basis of the VLAK protocol, was successfully achieved through suitable synthetic pathways, as shown in Scheme 3.

The derivatives **2aF** and **3aF** were synthesized in three preparative steps. The intermediates **2aB** and **3aB** were obtained, at first in very low yields, by reaction of the sodium salt of **2a** and **3a**, generated *in situ* using sodium hydride as base, and ethyl 4-bromobutyrate in dry DMF (*N*,*N*-DiMethylFormamide) at 80 °C. The use of potassium carbonate (5-fold excess of the starting material), at 60 °C, increased the yields up to 63%. Then the hydrolysis with NaOH in a solvent mixture EtOH/H_2O, quantitatively yielded the corresponding carboxylic acids **2aC** and **3aC**.

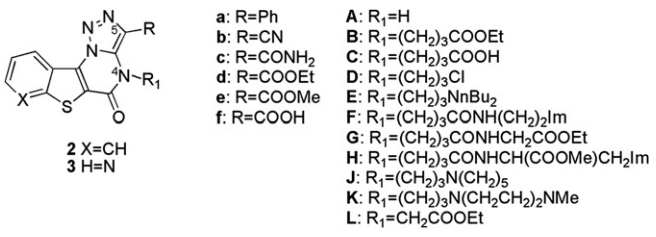

Fig. 4. Annelated thienotriazolopyrimidines *in house* database submitted to VLAK protocol.

Table 3
In house database virtual screening selected hits.

ID	[a]MA (A%)					
	A	**B**	**C**	**D**	**E**	**F**
2aF	38	**86**	45	78	51	31
3aE	42	**86**	38	70	47	36
3aF	33	76	49	**86**	53	33
3aK	40	**86**	47	69	55	33

[a] **A%**: percentage of affinity; **MA**, mechanism of action: **A**, Alkylating Agents; **B**, Antimitotic Agents; **C**, Topoisomerase I Inhibitors; **D**, Topoisomerase II Inhibitors; **E**, RNA/DNA Antimetabolites; **F**, DNA Antimetabolites. In bold are reported the highest A% values for the selected compounds.

Compounds **2aF** and **3aF** were suitably prepared by amidation of the acids **2aC** and **3aC** with histamine, in dioxane, in the presence of CDI (1,1′-carbonyldiimidazole) as coupling agent. A significant yield increase was obtained through the reaction with DMAP (4-DiMethylAminoPyridine) and EDCI (1-Ethyl-3-[3-Dimethylamino-propyl]CarbodiImide) (up to 75%) [24].

Derivative **3aE** was synthesized in two steps. The reaction of **3a** and 1-bromo-3-chloropropane gave the derivative **3aD** in low yield. From this last derivative, upon heating under reflux in dibutylamine solvent free, **3aE** was obtained.

Derivative **3aK** was prepared reacting in turn the intermediate **3aD** with *N*-methylpiperazine solvent free.

2.3. Biological screening

All the new designed pyrrolo-pyrimidines **2aF**, **3aE**, **3aK**, **3aF**, and the intermediates **2aB**, **2aC**, **3aB**, **3aC**, **3aD**, were subjected to the NCI disease-oriented human cell lines screening assay to be evaluated for their *in vitro* antitumor activity.

The derivatives **2aC**, **2aF**, **3aB**, **3aC**, **3aD**, **3aE**, **3aF**, and **3aK**, passed the selection criteria adopted by DTP NCI screening data and consequently were *in vitro* analyzed.

A single dose (10 μM) of the accepted compounds was tested against a panel of approximately 60 tumor human cell lines grouped in nine disease subpanels, including breast, central nervous system, colon, leukemia, melanoma, nonsmall-cell lung, ovarian, renal, and prostate tumors cell lines (Table 4, Supplementary material) [25–27].

In this biological protocol, each cell line is inoculated and pre-incubated on a microtiter plate. Test agents were then added at a single concentration and the culture is incubated for 48 h. End-point determinations were made with alamar blue [28]. Results for each tested agent are reported as the percent of growth (G%) of the treated cells when compared to the untreated control cells. Compounds that reduced the growth of any one of the cell lines to approximately 32% or less are passed on for evaluation in the full panel of 60 cell lines over a 5-log dose range.

Table 4
Overview of one dose screening for all sub-panels (G%).

PANEL	Derivative ([a]$G\%_a$)							
	2aC	**2aF**	**3aB**	**3aC**	**3aD**	**3aE**	**3aF**	**3aK**
Breast cancer	87	−5	96	106	105	106	79	−23
CNS cancer	87	−18	88	105	101	99	60	−43
Colon cancer	95	−49	82	109	91	97	49	−37
Leukemia	93	71	79	98	88	99	61	−22
Melanoma	94	−57	92	102	96	80	71	−78
Non-small cell lung cancer	91	−26	92	103	98	87	88	14
Ovarian cancer	92	−16	94	110	106	99	59	7
Prostate cancer	89	−41	99	109	95	103	46	39
Renal cancer	82	−34	94	111	98	76	79	−14
[b]Mean	90	**−21**	90	106	98	91	**69**	**−23**

[a] Cellular growth percentage average.
[b] In bold the G% mean of compounds passed on for evaluation in the full panel of 60 cell lines over a 5-log dose range.

The new annelated thienotriazolopyrimidines generally exhibited an excellent antiproliferative activity. In particular the derivatives **2aF**, **3aF**, and **3aK**, showed $G\%_a$ mean values of −21, 69, −23, respectively (Table 4).

These last derivatives exhibited $G\%_a$ values significantly under the level of 32% for at least one tumor cell line. Thus, according with the selection criteria of DTP NCI protocol, they were passed to five dose concentrations screening.

In the five dose screening, the antitumor activity is given by three parameters for each cell line: pGI_{50} value (GI_{50} is the molar concentration of the compound that inhibits 50% net cell growth), pTGI value (TGI is the molar concentration of the compound leading to total inhibition of net cell growth), and pLC_{50} value (LC_{50} is the molar concentration of the compound that induces 50% net cell death). Moreover, a Mean Graph MIDpoint (MG_MID) is calculated for each of the mentioned parameters, giving an average activity parameter overall cell lines. For the calculation of the MG_MID, insensitive cell lines are included with the highest concentration tested. The discovery of compounds with new selectivity patterns is

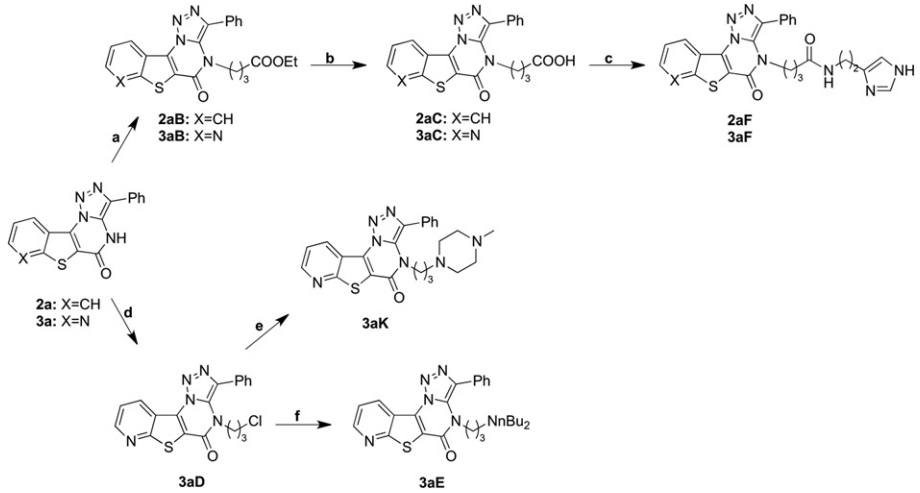

Scheme 3. Reaction steps leading to derivatives **2aF**, **3aE**, **3aK**, and **3aF** selected by VLAK protocol. Reagents and conditions: (a) K_2CO_3, DMF, Ethyl 4-Bromobutyrate; (b) NaOH, EtOH/H_2O; (c) Dioxane, DMAP/EDCI, histamine/TEA; (d) 1-Bromo-3-Chloropropane, K_2CO_3, DMF; (e) 1-methylpiperazine; (f) Dibutylamine, Δ.

Table 5
Overview of five dose screening tests results for **2aF**, **3aF**, **3aK** derivatives (Supplementary material).

Compd	pGI_{50}			pTGI			pLC_{50}		
	#	Range	MG_MID	#	Range	MG_MID	#	Range	MG_MID
2aF	54	4.73–6.74	5.81	52	<4.00–5.78	5.29	44	<4.00–5.35	4.62
3aF	59	4.47–7.02	5.29	59	<4.00–5.35	4.58	59	<4.00–4.41	4.15
3aK	59	5.03–6.80	5.30	59	4.75–5.76	4.94	59	4.39–5.42	4.60

[#]Number of cell lines investigated.

one of the targets of the DTP screening program. Selectivity of a compound with respect to a certain cell line of the screen is characterized by a high deviation of the particular cell line parameter compared to the MG_MID value. The overview of pGI_{50}, pTGI, and pLC_{50} values are reported in Table 5, together with the number of human tumor cell lines investigated.

An evaluation of the data reported in Supplementary material (Table S2) revealed that all the derivatives selected for the five dose screening, showed a significant antiproliferative activity against all the human tumor cell lines investigated, generally up to sub-micromolar concentration.

Considering the MG_MID values, in the range 5.29–5.81 for pGI_{50}, 4.58–5.29 for pTGI, and 4.15–4.62 for pLC_{50} (Table 5), the most active compound of the series resulted derivative **2aF**, at both pGI_{50} and pTGI level (5.81, 5.29), followed by **3aF**, and **3aK**. With respect to the tumor subpanels (Table S2), **2aF** resulted particularly effective against colon cancer and leukemia ones: in fact, the calculated pGI_{50} MG_MID values for these sub-panels (6.04 and 6.05, respectively) were always much higher than the overall cell lines MG_MID value (6.28). Remarkable was also the activity toward the ovarian subpanel, with pGI_{50} MG_MID value = 5.81. With respect to a particular cell line, **2aF** showed an excellent response against the SF-539 (CNS, $pGI_{50} = 6.18$), K-562 (leukemia, $pGI_{50} = 6.36$), CAKI-1 and SN12C (renal, $pGI_{50} = 6.74$ and 6.57, respectively).

Moreover, it has to be underlined the anticancer activity of **2aF** on the HCT-116 (colon) and OVCAR-8 (ovarian) with a $pGI_{50} = 6.47$ and 6.49, respectively, and $pLC_{50} < 4$, demonstrating the high potency and low toxicity of the compound. It is also of remarkable interest in the case of **2aF**, the appreciable number of cell lines with $pLC_{50} < 4$, (19/44), a result that can give account of the low toxicity of such a compound.

Finally, also the results of biological screenings on compound **3aF** need some considerations. Although the derivative was the least effective among those tested (MG_MID value = 5.29), it exhibited remarkable antiproliferative effect against at least seven cell lines (GI_{50} in the low micromolar range, from 3.8×10^{-7} to 9.5×10^{-8} M). In particular SF-539 (CNS, $pGI_{50} = 6.50$), CCRF-CEM (leukemia, $pGI_{50} = 6.65$), SN12C (renal, $pGI_{50} = 6.48$), and OVCAR-8 (ovarian, $pGI_{50} = 7.02$) cell lines resulted the more susceptible.

3. Conclusions

In this work, the combined use of the chemometric protocol Virtual Lock-and-Key (VLAK) and the synthetic procedures, well optimized by us for the building of heterocyclic compounds, allowed to identify annelated thienotriazolopyrimidines with antitumor activity up to sub-micromolar concentration. The derivative *N*-(2-(1*H*-Imidazol-4-yl)ethyl)-4-(5-oxo-3-phenylbenzo[4,5]thieno[2,3-*e*][1,2,3]triazolo[1,5-*a*]pyrimidin-4(5*H*)-*yl*)butanamide (**2aF**) revealed to be an excellent candidate as antitumor agent. In fact, it showed antiproliferative activity against all the fifty-six tumor cell lines tested, up to sub-nanomolar concentration. It is also of remarkable interest the appreciable number of cell lines with $pLC_{50} < 4$, (19/44), a result that can give account of the low toxicity of such a compound.

Also the thioisostere **3aF** exhibited remarkable antiproliferative effect against at least seven cell lines (GI_{50} in the low micromolar range, from 3.8×10^{-7} to 9.5×10^{-8} M). In particular SF-539 (CNS, $pGI_{50} = 6.50$), CCRF-CEM (leukemia, $pGI_{50} = 6.65$), SN12C (renal, $pGI_{50} = 6.48$), and OVCAR-8 (ovarian, $pGI_{50} = 7.02$) cell lines resulted the more susceptible.

If we analyze the antiproliferative profile of the tested compounds from the point of view of their structural features, it is possible to evidence as a basic chain [methylpiperazine (type K) or histamine (type F)] is necessary for a significant increase of the biological activity. Moreover also the core ring system resulted crucial for the modulation of biological aspects: the benzothieno bicycle was more effective of the isostere pyridothieno one.

4. Experimental

4.1. Computational details

The compounds of the NCI ACAM database [26–28], were drawn and optimized *in vacuo* by ligprep of MAESTRO SUITE [29]. The entries containing cations or consisting of a mix of two structures were excluded. Thus, the starting database was constituted from 114 compounds classified in six mechanism of action: 30, Alkylating Agents; 13, Antimitotic Agents; 24, Topoisomerase I Inhibitors; 15, Topoisomerase II Inhibitors; 16, RNA/DNA Antimetabolites; 16, DNA Antimetabolites (Supplementary material).

CODESSA PRO software was used for the molecular descriptors calculation [30]. For all structures 172 molecular descriptors belonging to different classes were calculated (Supplementary material).

In particular, for each class of drugs with known mechanism of action (Fig. 5a), the lock model was set as a sequence of molecular descriptor value ranges. Each range was defined as $\mu Dj(MA) \pm \sigma Dj(MA)$, where $\mu Dj(MA)$ is the molecular descriptor average value and $\sigma Dj(MA)$ is the standard deviation (Fig. 5b).

When the molecular descriptor value Dj of a tested structure T (Fig. 5c) falls within the defined range ($\mu Dj \pm \sigma Dj$) $\alpha = 1$ (Fig. 5d, i.e. D1, D3, and Dj), otherwise $\alpha = 0$ (i.e. D2, D4). At the end each tested structure is converted in a binary sequence (Supplementary material).

In the proposed protocol, it was supposed that the higher is the number of fitted molecular descriptors ($\alpha = 1$), the higher will be the potential anticancer capability of the investigated compound. Thus, the percentage of affinity A% (eq. (1)) was defined for each class (MA) as:

$$A\% = \sum \alpha i,j(MA)/D_{tot}*100 \quad (1)$$

Where $\Sigma\alpha i,j(MA)$ is the sum of all fitted molecular descriptors for the MA class and D_{tot} is the total of the molecular descriptors used in the VLAK protocol.

4.2. Chemistry

Unless otherwise indicated, all reagents and solvents were purchased from commercial sources and used without further

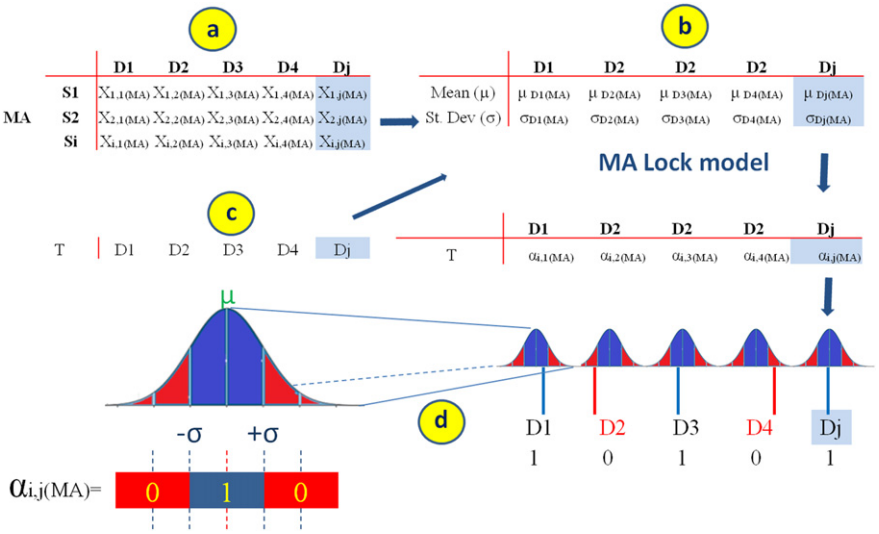

Fig. 5. VLAK protocol applied on NCI ACAM database. MA, mechanism of action; D_j, molecular descriptors; S_i, structures; T, *in silico* screened entry.

purification. All melting points (°C) were determined on a Büchi–Tottoli capillary apparatus and are uncorrected; IR spectra were determined in bromoform with a Jasco FT/IR 5300 spectrophotometer. ^{1}H NMR, ^{13}C NMR spectra were recorded in DMSO-d_6 solution, unless otherwise specified, at 200 and 50.3 MHz, respectively, using a Bruker AC-E series 200 MHz spectrometer. Chemical shifts values are given in ppm and referred as the internal standard to TMS (tetramethylsilane). The following abbreviations are used: br = broad signal, s = singlet, d = doublet, t = triplet, q = quartet, m = multiplet. The purity of all compounds screened in biological assays was determined to be >95% by HPLC/MS analysis. Mass spectroscopy was performed using a GC–MS Shimadzu QP5050 with EI (75ev). Microanalyses were in agreement with theoretical values ±0.4%. Thin layer chromatography was performed on precoated (0.25 mm) silica gel GF_{254} plates, compounds were detected with 254 nm UV lamp. Column chromatography was performed with Merck silica gel ASTM (230–400 mesh), or Merck aluminum oxide 90 (70–230 mesh), and with a Biotage FLASH40i chromatography module (prepacked cartridge system). The Ethyl 3-Aminobenzo[*b*]thiophene-2-carboxylate (**8**) is commercially available.

4.2.1. Synthesis of ethyl 3-azido-benzo[b]thiophene-2-carboxylate (*5*)

A solution of ethyl 3-amino-benzo[*b*]thiophene-2-carboxylate (**8**) (0.50 g, 2.3 mmol) in acetic acid (6 mL), was cooled in an ice bath to −5 °C. Then, a solution of sodium nitrite (0.32 g, 4.6 mmol), in water (2 mL), was slowly added, under vigorous stirring. After 30 min, sodium azide (0.60 g, 9.2 mmol) in water (2 mL), was added over 10 min. The reaction mixture was stirred for further 3 h at room temperature and then slowly poured onto water/ice. The precipitate was collected by filtration to give **5**, 0.40 g. Yield 70%. Mp 100 °C (dec). IR: 2130 (N_3), 1689 (CO) cm^{-1}. ^{1}H NMR δ: 1.30 (t, J = 7.1 Hz, 3H), 4.33 (q, J = 7.1 Hz, 2H), 7.34–7.51 (m, 2H), 7.88 (d, J = 8.1 Hz, 1H), 8.14 (d, J = 7.7 Hz, 1H). ^{13}C NMR δ: 14.4 (q), 59.7 (t), 122.9 (d), 123.0 (d), 123.8 (d), 128.4 (d), 131.5 (s), 133.7 (s), 138.8 (s), 149.7 (s), 164.5 (s). Elem. Anal. calcd. for $C_{11}H_9N_3O_2S$: C, 53.43; H, 3.67; N, 16.99; found: C, 53.62; H, 3.55; N, 17.30.

4.2.2. Synthesis of ethyl 3-aminothieno[2,3-b]pyridine-2-carboxylate (*9*)

According to the literature procedure [19], ethyl thioglycolate (1.2 mL, 11 mmol) was added to a stirred mixture of NaH 60% dispersion in mineral oil (0.36 g, 15 mmol) and dry dimethylsulfoxide (DMSO) (10 mL). After stirring at room temperature for 15 min, a solution of 2-chloro-3-cyanopyridine (1.40 g, 10 mmol) in dry DMSO (20 mL) was added dropwise. The reaction was stirred at room temperature for further 3 h and then was poured onto stirred water/ice. The light yellow precipitate was collected by filtration and dried to give **9**, 2.22 g. Yield 100%. Mp 183–184 °C. IR: 3487, 3395, (NH_2), 1689 (CO) cm^{-1}. ^{1}H NMR δ: 1.29 (t, J = 7.1 Hz, 3H), 4.30 (q, J = 7.1 Hz, 2H), 7.31 (br s, 2H), 7.46 (dd, J = 4.6, 8.2 Hz, 1H), 8.54 (dd, J = 1.6, 8.2 Hz, 1H), 8.68 (dd, J = 1.6, 4.6 Hz, 1H). ^{13}C NMR δ: 14.4 (q), 59.9 (t), 93.3 (s), 119.3 (d), 125.5 (s), 131.4 (d), 147.7 (s), 150.7 (d), 159.6 (s), 164.3 (s).

4.2.3. Synthesis of ethyl 3-azidothieno[2,3-b]pyridine-2-carboxylate (*6*)

A solution of ethyl 3-aminopyrido[3,2-*b*]thiophene-2-carboxylate (**9**) (0.3 g, 1.35 mmol) in 6 N hydrochloric acid (12 mL) was cooled in an ice bath to −5 °C. Then, a solution of sodium nitrite (0.186 g, 2.7 mmol) in water (2 mL) was added slowly, under vigorous stirring. After 30 min sodium azide (0.35 g, 5.4 mmol) in water (2 mL) was added dropwise over 10 min. The reaction mixture was stirred for further 3 h at room temperature and then slowly poured onto water/ice. The precipitate was collected by filtration, and dried in the absence of light to give **6**, 0.22 g. Yield 60%. Mp 93–94 °C. IR: 2127 (N_3), 1705 (CO) cm^{-1}. ^{1}H NMR δ: 1.30 (t, J = 7.1 Hz, 3H), 4.30 (q, J = 7.1 Hz, 2H), 7.46 (dd, J = 4.5, 8.2 Hz, 1H), 8.54 (dd, J = 1.6, 8.2 Hz, 1H), 8.68 (dd, J = 1.6, 4.5 Hz, 1H). ^{13}C NMR δ: 14.41 (q), 59.9 (t), 93.3 (s), 119.3 (d), 125.5 (s), 131.4 (d), 147.7 (s), 150.7 (d), 159.6 (s), 164.3 (s). Elem. Anal. calcd. for $C_{10}H_8N_3O_2S$: C, 48.38; H, 3.25; N, 22.75; found: C, 48.42; H, 3.27; N, 22.36.

4.2.4. General procedure for the preparation of benzothieno[2,3-e][1,2,3]triazolo[1,5-a]pyrimidines *2a,b*

The appropriate acetonitrile (1.73 mmol) in dry ethanol (2 mL) was added to a solution of 1.3 M sodium ethoxide in ethanol (2.7 mL), at room temperature. After 15 min of stirring, the reaction mixture was added to a solution of azido derivative **5** (0.215 g, 0.87 mmol) in dry ethanol (3 mL) and the mixture was stirred overnight at room temperature. Evaporation of the solvent under reduced pressure gave a crude which was purified by column chromatography using dichloromethane/methanol 9:1 as eluent.

4.2.5. 3-Phenylbenzo[4,5]thieno[2,3-e][1,2,3]triazolo[1,5-a] pyrimidin-5(4H)-one (**2a**)

Yellow solid, 0.18 g. Yield 65%. Mp > 300 °C. IR: 3401 (NH), 1651 (CO) cm^{-1}. ^1H NMR δ: 7.21 (t, $J = 7.4$ Hz, 1H), 7.40–7.62 (m, 4H), 7.97 (d, $J = 7.4$ Hz, 1H), 8.33 (d, $J = 7.4$ Hz, 1H), 8.54 (d, $J = 8.1$ Hz, 2H). ^{13}C NMR δ: 123.3 (d), 123.7 (d), 124.0 (d), 124.4 (d), 125.2 (d), 128.4 (d), 128.6 (d), 128.7 (s), 133.5 (s), 133.6 (s), 135.1 (s), 141.0 (s), 144.6 (s), 152.4 (s), 154.6 (s). Elem. Anal. calcd. for $C_{17}H_{10}N_4OS$: C, 64.14; H, 3.17; N, 17.50; found: C, 64.13; H, 3.25; N, 17.78.

4.2.6. 5-Oxo-4,5-dihydrobenzo[4,5]thieno[2,3-e][1,2,3]triazolo[1,5-a]pyrimidine-3-carbonitrile (**2b**)

Yellow solid, 0.14 g. Yield 60%. Mp > 300 °C. IR: 3321 (NH), 2240 (CN), 1656 (CO) cm^{-1}. ^1H NMR δ: 6.64–6.81 (m, 2H), 7.18 (d, $J = 8.0$ Hz, 1H), 7.44 (d, $J = 7.3$ Hz, 1H). ^{13}C NMR δ: 104.2 (s), 106.6 (s), 114.9 (s), 123.7 (d), 123.8 (d), 124.7 (d), 129.2 (d), 134.2 (s), 141.1 (s), 149.7 (s), 152.2 (s), 155.2 (s). Elem. Anal. calcd. for $C_{12}H_5N_5OS$: C, 53.93; H, 1.89; N, 26.20; found: C, 53.84; H, 1.93; N, 26.58.

4.2.7. General procedure for the preparation of Pyrido[3′,2′:4,5] thieno[2,3-e][1,2,3]triazolo[1,5-a]pyrimidines **3a**,**b**

The appropriate acetonitrile (1.73 mmol) in dry ethanol (2 mL) was added to a solution of 1.3 M sodium ethoxide in dry ethanol (2.7 mL), at room temperature. After 15 min of stirring, the reaction mixture was added to a solution of azido derivative **6** (0.215 g, 0.87 mmol) in dry ethanol (3 mL) and the mixture was stirred overnight at room temperature. Evaporation of the solvent under reduced pressure gave a crude which was purified by column chromatography using dichloromethane/methanol 9:1 as eluent.

4.2.8. 3-Phenylpyrido[3′,2′:4,5]thieno[2,3-e][1,2,3]triazolo[1,5-a] pyrimidin-5(4H)-one (**3a**)

Yellow solid, 0.17 g. Yield 63%. Mp > 300 °C. IR: 3368 (NH), 1630 (CO) cm^{-1}. ^1H NMR δ: 7.25 (d, $J = 7.8$ Hz, 1H), 7.44–7.60 (m, 3H), 7.96 (d, $J = 7.8$ Hz, 1H), 8.52–8.75 (m, 4H). ^{13}C NMR δ: 120.0 (d), 124.1 (d), 125.3 (d), 128.3 (d), 129.2 (d), 131.2 (s), 131.3 (d), 132.3 (s), 133.3 (s), 144.2 (s), 146.2 (s), 150.3 (d), 151.8 (s), 151.9 (s), 162.3 (s). Elem. Anal. calcd. for $C_{16}H_9N_5OS$: C, 60.18; H, 2.84; N, 21.93; found: C, 60.28; H, 2.63; N, 21.56.

4.2.9. 5-Oxo-4,5-dihydropyrido[3′,2′:4,5]thieno[2,3-e][1,2,3]triazolo [1,5-a]pyrimidine-3-carbonitrile (**3b**)

White solid, (0.14 g). Yield 60%. Mp > 300 °C. IR: 3404 (NH), 2231 (CN), 1685 (CO) cm^{-1}. ^1H NMR δ: 7.6 (dd, $J = 6.5$, 8.1 Hz, 1H), 8.65 (dd, $J = 3.2$, 8.1 Hz, 1H), 8.79 (dd, $J = 3.2$, 6.5 Hz, 1H), 8.85 (br s, 1H). ^{13}C NMR δ: 104.4 (s), 105.2 (s), 114.7 (s), 120.3 (s), 128.3 (d), 131.9 (d), 149.5 (s), 150.9 (d), 151.9 (s), 152.7 (s), 162.2 (s). Elem. Anal. calcd. for $C_{11}H_4N_6OS$: C, 49.25; H, 1.50; N, 31.33; found: C, 49.27; H, 1.43; N, 31.75.

4.2.10. Ethyl 3-(5-amino-4-cyano-1H-1,2,3-triazol-1-yl)thieno[2,3-b]pyridine-2-carboxylate (10, X = N, R = CN)

By identical synthetic procedure used for **3b**, reducing the solvent volume (2 mL), the intermediate **10** (X = N, R = CN) was filtered off, air dried and recrystallized from ethanol. Yellow solid, 0.093 g. Yield 35%. Mp > 300 °C. IR: 3550, 3420 (NH_2), 2254 (CN), 1648 (CO) cm^{-1}. ^1H NMR δ: 1.39 (t, $J = 7.0$ Hz, 3H), 4.35 (q, $J = 7.0$ Hz, 2H), 7.60 (dd, $J = 4.6$, 7.9 Hz, 1H), 8.63 (dd, $J = 1.6$, 7.9 Hz, 1H), 8.77 (dd, $J = 1.6$, 4.6 Hz, 1H), 8.89 (s, 2H). ^{13}C NMR δ: 14.4 (t), 59.5 (t), 103.8 (s), 120.2 (d), 122.5 (s), 128.6 (s), 131.5 (d), 146.7 (s), 150.7 (d), 152.1 (s), 152.3 (s), 161.3 (s), 162.3 (s). Elem. Anal. calcd. for $C_{13}H_{10}N_6O_2S$: C, 49.67; H, 3.21; N, 26.74; found: C, 49.88; H, 3.38; N, 26.33.

4.2.11. General procedure for the preparation of ethyl butanoate derivatives **2aB**, **3aB**

To a stirred suspension of **2a** or **3a** (1.0 mmol) in dry *N*,*N*-dimethylformamide (5 mL), potassium carbonate (3.0 mmol) and ethyl 4-bromobutyrate (5.0 mmol) were added. The mixture was heated at 60 °C for 16 h, cooled to room temperature, and then slowly poured onto water/ice. The crude solid was filtered and purified by column chromatography using dichloromethane/ethyl acetate 95:5 as eluent.

4.2.12. Ethyl 4-(5-oxo-3-phenylbenzo[4,5]thieno[2,3-e][1,2,3] triazolo[1,5-a]pyrimidin-4(5H)-yl)butanoate (**2aB**)

Purified by column chromatography using dichloromethane/petroleum ether 98:2 as eluent to afford **2aB**, 0.17 g. Yield 40%. Mp 123.6–124.0 °C. IR: 1725, 1677 (CO) cm^{-1}. ^1H NMR ($CDCl_3$) δ: 1.22 (t, $J = 7.4$ Hz, 3H), 2.07–2.15 (m, 2H), 2.41 (t, $J = 7.2$ Hz, 2H), 4.08 (q, $J = 7.4$ Hz, 2H), 5.04 (t, $J = 7.2$ Hz, 2H), 7.49–7.62 (m, 5H), 7.90 (d, $J = 7.4$ Hz, 1H), 8.48 (d, $J = 7.4$ Hz, 1H), 8.60 (d, $J = 8.0$ Hz, 2H). ^{13}C NMR ($CDCl_3$) δ: 14.1 (q), 23.6 (t), 31.1 (t), 55.3 (t), 60.7 (t), 115.7 (s), 123.4 (d), 124.3 (d), 125.0 (d), 127.0 (d), 128.6 (s), 128.8 (d), 129.5 (d), 129.9 (d), 134.1 (s), 139.2 (s), 142.1 (s), 145.9 (s), 152.0 (s), 155.5 (s), 172.2 (s). Elem. Anal. calcd. for $C_{23}H_{20}N_4O_3S$: C, 63.87; H, 4.66; N, 12.95; found: C, 63.61; H, 4.83; N, 12.54.

4.2.13. Ethyl 4-(5-oxo-3-phenylpyrido[3′,2′:4,5]thieno[2,3-e][1,2,3] triazolo[1,5-a]pyrimidin-4(5H)-yl)butanoate (**3aB**)

Purified by column chromatography using dichloromethane/ethyl acetate 98:2 as eluent to afford **3aB**, 0.27 g. Yield 63%. Mp 109.6–110.8 °C. IR: 1723, 1683 (CO) cm^{-1}. ^1H NMR δ: 1.08 (t, $J = 7.1$ Hz, 3H), 2.06 (m, 2H), 2.41 (t, $J = 7.2$ Hz, 2H), 3.93 (q, $J = 7.1$ Hz, 2H), 4.94 (t, $J = 6.6$ Hz, 2H), 7.50–7.63 (m, 4H), 8.42 (d, $J = 8.1$ Hz, 2H), 8.61 (dd, $J = 2.0$, 7.7 Hz, 1H), 8.77 (dd, $J = 1.6$, 6.9 Hz, 1H). ^{13}C NMR δ: 13.9 (q), 23.6 (t), 30.3 (t), 55.2 (t), 59.9 (t), 112.6 (s), 120.8 (d), 126.2 (d), 127.5 (s), 128.1 (s), 128.8 (d), 129.6 (s), 131.9 (d), 136.6 (s), 145.3 (s), 150.8 (d), 151.6 (d), 152.0 (s), 161.7 (s), 172.0 (s). Elem. Anal. calcd. for $C_{22}H_{20}N_5O_3S$: C, 60.96; H, 4.42; N, 16.16; found: C, 60.67; H, 4.51; N, 16.38.

4.2.14. General procedure for the preparation of **2aC** and **3aC**

To a stirred suspension of the carboxyethyl derivate (**2aB**, **3aB**) (0.5 mmol) in dry ethanol (5 mL), a solution of potassium hydroxide (0.13 g, 2.5 mmol) in water (2 mL) was added dropwise. The mixture was stirred at room temperature for 1–8 h. The ethanol was evaporated under reduced pressure. The residue was dissolved in water (10 mL) and then carefully adjusted to pH = 1 with 6 N hydrochloric acid. The precipitate was filtered off, air dried and recrystallized from ethanol to afford the corresponding acid.

4.2.15. 4-(5-Oxo-3-phenylbenzo[4,5]thieno[2,3-e][1,2,3]triazolo [1,5-a]pyrimidin-4(5H)-yl)butanoic acid (**2aC**)

The recrystallization from ethanol affords **2aC** as white solid, 0.40 g. Yield 100%. Mp 219.3–220.0 °C. IR: 3520–2900 (OH), 1754, 1679 (CO) cm^{-1}. ^1H NMR δ: 2.09–2.16 (m, 2H), 2.40 (t, $J = 7.4$ Hz, 2H), 5.01 (t, $J = 7.4$ Hz, 2H), 7.50–7.64 (m, 5H), 7.93 (d, $J = 7.4$ Hz, 1H), 8.40 (d, $J = 7.4$ Hz, 1H), 8.58 (d, $J = 8.0$ Hz, 2H), 9.98 (br s, 1H). ^{13}C NMR δ: 23.6 (t), 31.0 (t), 55.3 (t), 115.6 (s), 123.4 (d), 124.3 (d), 125.0 (d), 127.0 (d), 128.5 (s), 128.8 (d), 129.4 (d), 129.9 (d), 134.6 (s), 139.2 (s), 142.0 (s), 145.9 (s), 152.0 (s), 155.4 (s), 172.1 (s). Elem. Anal. calcd. for $C_{21}H_{16}N_4O_3S$: C, 62.36; H, 3.99; N, 13.85; found: C, 62.44; H, 4.16; N, 13.48.

4.2.16. 4-(5-Oxo-3-phenylpyrido[3′,2′:4,5]thieno[2,3-e][1,2,3] triazolo[1,5-a]pyrimidin-4(5H)-yl)butanoic acid (**3aC**)

The recrystallization from ethanol affords **3aC** as a white solid, 0.17 g. Yield 86%. Mp 171.0–171.6 °C. IR: 3490–2965 (OH), 1745, 1681 (CO) cm^{-1}. ^1H NMR δ: 1.99–2.13 (m, 2H), 2.30 (t, $J = 6.6$ Hz, 2H), 4.40 (t, $J = 6.6$ Hz, 2H), 7.27 (dd, $J = 4.5$, 8.4 Hz, 1H), 7.35–7.54 (m, 4H), 7.88 (dd, $J = 8.2$ Hz, 2H), 8.65 (dd, $J = 1.5$, 4.5 Hz, 1H), 9.33 (br s, 1H). ^{13}C NMR δ: 24.6 (t), 30.3 (t), 53.9 (t), 99.4 (s), 118.9 (s),

119.2 (d), 125.6 (s), 126.1 (d), 128.2 (d), 128.8 (d), 129.6 (s), 132.6 (d), 137.8 (s), 143.0 (s), 150.0 (d), 159.0 (s), 166.1 (s), 173.7 (s). Elem. Anal. calcd. for $C_{20}H_{15}N_5O_3S$: C, 59.25; H, 3.73; N, 17.27; found: C, 59.19; H, 3.56; N, 17.63.

*4.2.17. General procedure for the preparation of **2aF** and **3aF***

To a stirred suspension of the acid (**2a**C, **3aC**) (0.44 mmol) in dry dioxane (5 mL), DMAP (0.05 g, 0.45 mmol) and EDCI (0.17 g, 9.2 mmol) were added under nitrogen atmosphere, at 0 °C. After 2 h of stirring at room temperature, histamine (0.102 g, 9.2 mmol) was carefully added. The reaction mixture was incubated at 50 °C for 12 h. Then, the reaction solvent was evaporated under reduced pressure and the crude was purified by column chromatography using dichloromethane/methanol 9:1 as eluent.

*4.2.18. N-(2-(1H-Imidazol-4-yl)ethyl)-4-(5-oxo-3-phenylbenzo [4,5]thieno[2,3-e][1,2,3]triazolo[1,5-a]pyrimidin-4(5H)-yl) butanamide (**2aF**)*

White solid, 0.13 g. Yield 60%. Mp 171.2–171.6 °C. IR: 3360 (NH), 1720, 1680 (CO) cm^{-1}. ^1H NMR δ: 2.02–2.18 (m, 4H), 3.17 (t, $J = 7.4$ Hz, 2H), 3.45 (m, 2H), 4.96 (t, $J = 6.6$ Hz, 2H), 6.72 (s, 1H), 7.49–7.89 (m, 7H), 8.16 (d, $J = 6.9$ Hz, 1H), 8.45 (d, $J = 6.9$ Hz, 1H), 8.57 (d, $J = 7.4$ Hz, 2H). ^{13}C NMR δ: 24.1 (t), 26.9 (t), 32.0 (t), 38.7 (t), 55.5 (t), 123.7 (d), 124.0 (d), 124.1 (d), 125.5 (d), 126.5 (d), 128.5 (s), 128.9 (d), 129.7 (d), 129.8 (d), 133.6 (s), 134.6 (d), 137.0 (s), 137.2 (s), 141.0 (s), 151.3 (s), 153.9 (s), 154.5 (s), 170.7 (s), 171.2 (s). Elem. Anal. calcd. for $C_{26}H_{23}N_7O_2S$: C, 62.73; H, 4.66; N, 19.71; found: C, 62.62; H, 4.77; N, 19.35.

*4.2.19. N-(2-(1H-Imidazol-4-yl)ethyl)-4-(5-oxo-3-phenylpyrido [3′,2′:4,5]thieno[2,3-e][1,2,3]triazolo[1,5-a]pyrimidin-4(5H)-yl) butanamide (**3aF**)*

White solid, 0.14 g. Yield 75%. Mp 239.7–240.3 °C. IR: 3363 (NH), 1727, 1685 (CO) cm^{-1}. ^1H NMR δ: 2.00–2.21 (m, 4H), 3.14 (t, $J = 7.0$ Hz, 2H), 3.44 (t, $J = 6.5$ Hz, 2H), 5.00 (t, $J = 6.5$ Hz, 2H), 6.70 (s, 1H), 7.48 (s, 1H), 7.49–7.68 (m, 4H), 7.72 (dd, $J = 4.6$, 8.0 Hz, 1H), 8.57 (dd, $J = 1.6$, 8.3 Hz, 2H), 8.85–8.90 (m, 2H). ^{13}C NMR δ: 24.5 (t), 26.9 (t), 31.1 (t), 38.8 (t), 53.7 (t), 99.4 (s), 113.0 (d), 115.8 (s), 119.2 (d), 121.4 (s), 125.5 (s), 126.1 (d), 128.2 (d), 127.8 (d), 128.4 (d), 129.6 (s), 132.5 (d), 137.6 (s), 143.0 (s), 149.9 (d), 159.0 (s), 166.1 (s), 173.6 (s). Elem. Anal. calcd. for $C_{25}H_{22}N_8O_2S$: C, 60.23; H, 4.45; N, 22.48; found: C, 60.17; H, 4.51; N, 22.77.

*4.2.20. Procedure for the preparation of **3aD***

To a stirred suspension of **3aA** (0.62 g, 1.93 mmol) in dry *N*,*N*-dimethylformamide (12 mL), potassium carbonate (0.8 g, 5.81 mmol) and 1-bromo-3-chloropropane (1.52 g, 9.68 mmol) were added. The mixture was heated at 60 °C for 16 h, cooled to room temperature, and then slowly poured onto water/ice. The precipitate was purified by column chromatography using dichloromethane/ethyl acetate 98:2 as eluent.

*4.2.21. 4-(3-Chloropropyl)-3-phenylpyrido[3′,2′:4,5]thieno[2,3-e] [1,2,3]triazolo[1,5-a]pyrimidin-5(4H)-one (**3aD**)*

Pale yellow solid, 0.42 g. Yield 55%. Mp 200.8–201.7 °C. IR: 1645 (CO) cm^{-1} ^1H NMR ($CDCl_3$) δ: 2.28–2.43 (m, 2H), 3.63 (t, $J = 6.3$ Hz, 2H), 5.13 (t, $J = 6.3$ Hz, 2H), 7.47–7.57 (m, 4H), 8.56 (d, $J = 8.2$ Hz, 2H), 8.70 (dd, $J = 1.7$, 6.6 Hz, 1H), 8.79 (dd, $J = 1.7$, 4.6 Hz, 1H). ^{13}C NMR δ: 31.2 (t), 41.3 (t), 53.6 (t), 100.0 (s), 115.0 (s), 120.2 (d), 127.0 (d), 128.2 (s), 128.8 (d), 130.2 (d), 132.2 (d), 139.2 (s), 145.7 (s), 151.5 (d), 151.9 (s), 152.9 (s), 163.4 (s). Elem. Anal. calcd. for $C_{19}H_{14}ClN_5OS$: C, 57.65; H, 3.56; N, 17.69; found: C, 57.76; H, 3.39; N, 17.43.

*4.2.22. Procedure for the preparation of **3aK***

A stirred suspension of **3aD** (0.10 g, 0.25 mmol) in 1-methylpiperazine (3 mL) was heated at reflux for 2 h. After cooling the mixture was poured onto water/ice and the precipitate was filtered off.

*4.2.23. 4-(3-(4-Methylpiperazin-1-yl)propyl)-3-phenylpyrido [3′,2′:4,5]thieno[2,3-e][1,2,3]triazolo[1,5-a]pyrimidin-5(4H)-one (**3aK**)*

Purified by alumina column chromatography using dichloromethane/petroleum ether 98:2 as eluent to afford **3aK**, 0.10 g. Yield 85%. Mp 88.3–90.2 °C. IR: 1655 (CO) cm^{-1}. ^1H NMR ($CDCl_3$) δ: 1.90–2.03 (m, 2H), 2.14 (s, 3H), 2.28–2.43 (m, 10H), 5.12 (t, $J = 6.8$ Hz, 2H), 7.47–7.60 (m, 4H), 8.56 (d, $J = 8.0$ Hz, 2H), 8.72 (dd, $J = 1.4$, 7.4 Hz, 1H), 8.78 (dd, $J = 1.4$, 4.5 Hz, 1H). ^{13}C NMR ($CDCl_3$) δ: 26.1 (t), 45.9 (q), 53.0 (t), 53.2 (t), 54.7 (t), 55.1 (t), 99.7 (s), 120.2 (d), 126.9 (d), 128.3 (s), 128.5 (s), 128.8 (d), 129.8 (d), 132.1 (d), 138.2 (s), 145.2 (s), 151.4 (d), 151.7 (s), 152.9 (s), 163.4 (s). Elem. Anal. calcd. for $C_{24}H_{25}N_7OS$: C, 62.72; H, 5.48; N, 21.33; found C, 62.53; H, 5.66; N, 21.62.

*4.2.24. Procedure for the preparation of **3aE***

A stirred suspension of **3aD** (0.10 g, 0.25 mmol) in dibutylamine (3 mL) was heated at reflux for 2 h. After cooling the mixture was poured into water/ice and the precipitate was filtered off and purified by alumina column chromatography, using dichloromethane/ethyl acetate 98:2 as eluent.

*4.2.25. 4-(3-(Dibutylamino)propyl)-3-phenylpyrido[3′,2′:4,5] thieno[2,3-e][1,2,3]triazolo[1,5-a]pyrimidin-5(4H)-one (**3aE**)*

White solid, 0.08 g. Yield 67%. Mp 109.5–110.5 °C. IR: 1643 (CO) cm^{-1}. ^1H NMR δ: 0.86 (t, $J = 6.7$ Hz, 6H), 1.24–1.34 (m, 10H), 1.81–1.95 (m, 2H), 2.34 (t, $J = 6.7$ Hz, 4H), 2.49 (t, $J = 6.7$ Hz, 2H), 7.49–7.61 (m, 4H), 8.58 (dd, $J = 1.7$, 8.2 Hz, 2H), 8.73 (dd, $J = 1.7$, 7.9 Hz, 1H), 8.81 (dd, $J = 1.7$, 4.6 Hz, 1H). ^{13}C NMR δ: 13.0 (q), 20.6 (t), 26.3 (t); 29.1 (t), 50.8 (t), 53.7 (t), 55.1 (t), 120.1 (d), 126.9 (d), 128.3 (s), 128.5 (s), 128.8 (d), 129.8 (d), 132.1 (d), 138.4 (s), 145.2 (s), 145.8 (s), 151.4 (d), 151.7 (s), 152.9 (s), 163.4 (s). Elem. Anal. calcd. for $C_{27}H_{33}N_6OS$: C, 66.36; H, 6.60; N, 17.20; found C, 66.47; H, 6.84; N, 17.59.

4.3. Biology

The human tumor cell lines of the cancer screening panel are grown in RPMI 1640 medium containing 5% fetal bovine serum and 2 mM L-glutamine. For a typical screening experiment, cells are inoculated into 96 well microtiter plates in 100 μl at plating densities ranging from 5000 to 40,000 cells/well depending on the doubling time of individual cell lines. After cell inoculation, the microtiter plates are incubated at 37 °C, 5% CO_2, 95% air and 100% relative humidity for 24 h prior to addition of experimental drugs.

After 24 h, two plates of each cell line are fixed *in situ* with TCA, to represent a measurement of the cell population for each cell line at the time of drug addition (Tz). Experimental drugs are solubilized in dimethylsulfoxide at 400-fold the desired final maximum test concentration and stored frozen prior to use. At the time of drug addition, an aliquot of frozen concentrate is thawed and diluted to twice the desired final maximum test concentration with complete medium containing 50 μg/mL gentamicin. Additional four, 10-fold or ½ log serial dilutions are made to provide a total of five drug concentrations plus control. Aliquots of 100 μl of these different drug dilutions are added to the appropriate microtiter wells already containing 100 μl of medium, resulting in the required final drug concentrations.

Following drug addition, the plates are incubated for an additional 48 h at 37 °C, 5% CO_2, 95% air, and 100% relative humidity. For adherent cells, the assay is terminated by the addition of cold TCA. Cells are fixed *in situ* by the gentle addition of 50 μl of cold 50% (w/v) TCA (final concentration, 10% TCA) and incubated for 60 min at

4 °C. The supernatant is discarded, and the plates are washed five times with tap water and air dried. Sulforhodamine B (SRB) solution (100 μl) at 0.4% (w/v) in 1% acetic acid is added to each well, and plates are incubated for 10 min at room temperature. After staining, unbound dye is removed by washing five times with 1% acetic acid and the plates are air-dried. Bound stain is subsequently solubilized with 10 mM trizma base, and the absorbance is read on an automated plate reader at a wavelength of 515 nm. For suspension cells, the methodology is the same except that the assay is terminated by fixing settled cells at the bottom of the wells by gently adding 50 μl of 80% TCA (final concentration, 16% TCA). Using the seven absorbance measurements [time zero, (Tz), control growth, (C), and test growth in the presence of drug at the five concentration levels (Ti)], the percentage growth is calculated at each of the drug concentrations levels. Percentage growth inhibition is calculated as:

$$[(\mathrm{Ti}-\mathrm{Tz})/(\mathrm{C}-\mathrm{Tz})]\times 100 \text{ for concentrations for which } \mathrm{Ti}\geq \mathrm{Tz}$$

$$[(\mathrm{Ti}-\mathrm{Tz})/\mathrm{Tz}]\times 100 \text{ for concentrations for which } \mathrm{Ti}<\mathrm{Tz}.$$

Three dose response parameters are calculated for each experimental agent. Growth inhibition of 50% (GI_{50}) is calculated from $[(\mathrm{Ti}-\mathrm{Tz})/(\mathrm{C}-\mathrm{Tz})]\times 100 = 50$, which is the drug concentration resulting in a 50% reduction in the net protein increase (as measured by SRB staining) in control cells during the drug incubation. The drug concentration resulting in total growth inhibition (TGI) is calculated from Ti = Tz. The LC_{50} (concentration of drug resulting in a 50% reduction in the measured protein at the end of the drug treatment as compared to that at the beginning) indicating a net loss of cells following treatment is calculated from $[(\mathrm{Ti}-\mathrm{Tz})/\mathrm{Tz}]\times 100 = -50$. Values are calculated for each of these three parameters if the level of activity is reached; however, if the effect is not reached or is exceeded, the value for that parameter is expressed as greater or less than the maximum or minimum concentration tested.

Acknowledgments

Thanks are due to the NCI, Bethesda, MD (USA) for performing the antitumor testing of the synthesized compounds.

Appendix A. Supplementary material

Supplementary data related to this article can be found at http://dx.doi.org/10.1016/j.ejmech.2013.01.019.

References

[1] A.R. Katritzky, I. Tulp, D.C. Fara, A. Lauria, U. Maran, W.E. Acree, A general treatment of solubility. 3. Principal component analysis (PCA) of the solubilities of diverse solutes in diverse solvents, J. Chem. Inf. Model. 45 (2005) 913–923.
[2] A. Lauria, P. Diana, P. Barraja, A. Montalbano, G. Cirrincione, G. Dattolo, A.M. Almerico, MADoSPRO: a new Approach to molecular modelling studies on a series of DNA minor groove binders, QSAR Comb. Sci. 25 (2006) 252–262.
[3] A. Lauria, M. Ippolito, A.M. Almerico, Principal component analysis on molecular descriptors as an alternative point of view in the search of new Hsp90 inhibitors, J. Comp. Biol. Chem. 33 (2009) 386–390.
[4] A. Lauria, M. Ippolito, A.M. Almerico, Combined use of PCA and QSAR/QSPR to predict the drugs mechanism of action. An application to the NCI ACAM Database, QSAR Comb. Sci. 28 (2009) 387–395.
[5] A. Lauria, M. Tutone, A.M. Almerico, Virtual lock-and-key approach: the in silico revival of Fischer model by means of molecular descriptors, Eur. J. Med. Chem. 46 (2011) 4274–4280.
[6] E. Fischer, Influence of the configuration on the action of the enzymes, Ber. Dtsch. Chem. Ges. 27 (1894) 2985–2993.
[7] E. Fischer, Faraday lecture on "SYNTHETICAL chemistry in its relation to biology", J. Chem. Soc. 91 (1907) 1747–1765.
[8] E. Fischer, Bedeutung der Stereochemie fur die Physilogie Hoppe-Seyler's, Z. Physiol. Chem. 26 (1898) 82–83.
[9] A. Lauria, C. Patella, G. Dattolo, A.M. Almerico, Design and synthesis of 4-substituted indolo[3,2-*e*][1,2,3]triazolo[1,5-*a*]pyrimidine derivatives with antitumor activity, J. Med. Chem. 51 (2008) 2037–2046.
[10] A. Lauria, P. Diana, P. Barraja, A. Montalbano, G. Cirrincione, G. Dattolo, A.M. Almerico, New tricyclic systems of biological interest. Annelated 1,2,3-triazolo[1,5-*a*]pyrimidines through domino reaction of 3-azidopyrroles and methylene active nitriles, Tetrahedron 58 (2002) 9723–9727.
[11] A. Lauria, C. Patella, P. Diana, P. Barraja, A. Montalbano, G. Cirrincione, G. Dattolo, A.M. Almerico, New tetracyclic ring system of biological interest. Indolo[3,2-*e*][1,2,3]triazolo[1,5-*a*]pyrimidines through domino reaction of 2-azidoindole, Heterocycles 60 (2003) 2669–2675.
[12] A. Lauria, C. Patella, P. Diana, P. Barraja, A. Montalbano, G. Cirrincione, G. Dattolo, A.M. Almerico, A synthetic approach to new polycyclic ring system of biological interest through domino reaction: indolo[2,3-*e*][1,2,3]triazolo [1,5-*a*]pyrimidine, Tetrahedron Lett. 47 (2006) 2187–2190.
[13] A. Lauria, I. Abbate, C. Patella, N. Gambino, A. Silvestri, G. Barone, A.M. Almerico, Pyrazolo[3,4-*d*][1,2,3]triazolo[1,5-*a*]pyrimidine: a new ring system through Dimroth rearrangement, Tetrahedron Lett. 49 (2008) 5125–5128.
[14] A. Lauria, M. Bruno, P. Diana, P. Barraja, A. Montalbano, G. Cirrincione, G. Dattolo, A.M. Almerico, Annelated pyrrolo-pyrimidines from amino-cyano-pyrroles and BMMAs as leads for new DNA-interactive ring systems, Bioorg. Med. Chem. 13 (2005) 1545–1553.
[15] A. Lauria, A. Guarcello, G. Dattolo, A.M. Almerico, Bis-1,2,4-triazolo[4,3-a:3',4'-c]quinoxalines of pharmaceutical interest from 1,3-dipolar cycloaddition, Tetrahedron Lett. 49 (2008) 1847–1850.
[16] A. Lauria, A. Guarcello, G. Macaluso, G. Dattolo, A.M. Almerico, Reactivity of asymmetric benzo-condensed diazines with nitrilimine dipoles in the 1,3-dipolar cycloaddition reactions, Tetrahedron Lett. 50 (2009) 7333–7336.
[17] A. Lauria, A. Guarcello, G. Dattolo, A.M. Almerico, Study of reactivity in the 1,3-dipolar cycloaddition reactions leading to new triazolopyrrolopyrazine ring systems, Synlett 14 (2010) 2067–2070.
[18] N.T. Pokhodylo, V.S. Matiychuk, N.D. Obushak, Synthesis of a new heterocyclic system - pyrido[3',2':4,5]thieno[2,3-*e*][1,2,3]triazolo[1,5-*a*]pyrimidine, Chem. Heterocycl. Comp. 45 (2009) 881–883.
[19] H.D.H. Showalter, A.J. Bridges, H.R. Zhou, A.D. Sercel, A. McMichael, D.W. Fry, Tyrosine kinase inhibitors. 16. 6,5,6-tricyclic benzothieno [3,2-*d*]pyrimidines and pyrimido[5,4-*b*]- and -[4,5-*b*]indoles as potent inhibitors of the epidermal growth factor receptor tyrosine kinase, J. Med. Chem. 42 (1999) 5464–5474.
[20] A. Monks, D. Scudiero, P. Skehan, R. Shoemaker, K. Paull, D. Vistica, C. Hose, J. Langley, P. Cronise, A. Vaigro-Wolff, M. Gray-Goodrich, H. Campbell, J. Mayo, M. Boyd, Feasibility of a high-flux anticancer drug screen utilizing a diverse panel of human tumor cell lines in culture, J. Natl. Cancer Inst. 83 (1991) 757–766.
[21] J.N. Weinstein, K.W. Kohn, M.R. Grever, V.N. Viswanadhan, L.V. Rubinstein, A.P. Monks, D.A. Scudiero, L. Welch, A.D. Koutsoukos, A.J. Chiausa, K.D. Paull, Neural computing in cancer drug development: predicting mechanism of action, Science 258 (1992) 447–451.
[22] W.W. Osdol, T.G. Myers, K.D. Paull, K.W. Kohn, J.N. Weinstein, Use of the Kohonen self-organizing map to study the mechanisms of action of chemotherapeutic agents, J. Natl. Cancer Inst. 86 (1994) 1853–1859.
[23] A. Lauria, C. Patella, I. Abbate, A. Martorana, A.M. Almerico, Lead optimization through VLAK protocol: new annelated pyrrolo-pyrimidine derivatives as antitumor agents, Eur. J. Med. Chem. 55 (2012) 375–383.
[24] Y. Hirayama, T. Nakamura, S. Uehara, Y. Sakamoto, K. Yamaguchi, K. Sei, M. Iwamura, Synthesis and characterization of new polyester dendrimers from acetoacetate and acrylate, Org. Lett. 7 (2005) 525–528.
[25] M.R. Grever, S.A. Schepartz, B.A. Chabner, The National Cancer Institute: cancer drug discovery and development program, Semin. Oncol. 19 (1992) 622–638.
[26] A. Monks, D. Scudiero, P. Skehan, Feasibility of a high-flux anticancer drug screen using a diverse panel of cultured human tumor cell lines, J. Natl. Cancer Inst. 83 (1991) 757–766.
[27] P. Skehan, R. Storeng, D. Scudiero, A. Monks, J. McMahon, D. Vistica, J.R. Warren, H. Bokesch, S. Kenney, M.R. Boyd, New colorimetric cytotoxicity assay for anticancer-drug screening, J. Natl. Cancer Inst. 82 (1990) 1107–1112.
[28] G.D. Gray, E. Wickstrom, Evaluation of anchorage-independent proliferation in tumorigenic cells using the redox dye alamarblue[TM], BioTechniques 21 (1996) 780–782.
[29] LigPrep, Version 2.4, Schrödinger LLC, New York, NY, 2010.
[30] A.R. Katrinsky, V.S. Lobanov, M. Karelson, Quantum-chemical descriptors in QSAR/QSPR studies, Chem. Rev. 96 (1996) 1027–1043.